Mechanism of *Bacillus* 1,3-1,4-β-D-Glucan 4-Glucanohydrolases: Kinetics and pH Studies with 4-Methylumbelliferyl β-D-Glucan Oligosaccharides†

Carles Malet and Antoni Planas*

Laboratory of Biochemistry, Institut Químic de Sarrià, Universitat Ramon Llull, Via Augusta 390, 08017 Barcelona, Spain

Received May 14, 1997; Revised Manuscript Received July 29, 1997⊗

ABSTRACT: The carbohydrate binding site of *Bacillus licheniformis* 1,3-1,4-β-D-glucan 4-glucanohydrolase was probed with a series of synthetic 4-methylumbelliferyl β-D-glucan oligosaccharides (**1a**−**e**). The title enzyme is a retaining *endo*-glycosidase that has an extended carbohydrate binding site composed of four glucopyranosyl binding subunits on the non-reducing end from the scissile glycosidic bond, plus two or three subsites on the reducing end. Subsites −II to −IV have a stabilizing effect on the enzyme−substrate transition state complex in the rate-determining step leading to a glycosyl−enzyme intermediate, with subsite −III having a larger effect (−3.5 kcal mol^{-1}). Since K_M values decrease from the mono- to the tetrasaccharide, part of the effect is due to ground stabilization of the Michaelis complex. On the other hand, the chromophoric trisaccharide **1c** and the homologous nonchromogenic tetrasaccharide **2b**, which locates a glucopyranosyl unit in subsite +I, have almost identical K_M values, the difference in reactivity being a consequence of an 18-fold increase of k_{cat} for **2b**. Therefore, interactions between subsite +I and the substrate appear to be mainly used to lower the energy of the transition state in the glycosylation step, rather than in the stabilization of the Michaelis complex. Finally, the pH dependence of the kinetic parameters for the hydrolysis of **1c**, and the pH-dependent enzyme inactivation by a water-soluble carbodiimide (EAC) suggest two essential groups with pK_a values of 5.5 and 7.0 in the free enzyme. The latter value is shifted up to 1.5 pH units upon binding of substrate in the non-covalent enzyme−substrate complex.

1,3-1,4-β-D-Glucan 4-glucanohydrolases (1,3-1,4-β-glucanase,[1] EC 3.2.1.73) are glycosidases that catalyze the hydrolysis of β-glucans containing mixed β-1,3 and β-1,4 glycosidic linkages, such as cereal β-glucans and lichenan. Cleavage of the natural substrates occurs regiospecifically on β-1,4-glycosidic linkages in 3-*O*-substituted glucopyranose units, as deduced from the structures of the final reaction products (*1*−*3*).

The 1,3-1,4-β-glucanases cloned so far belong to two distinct families, plant and microbial enzymes, with neither sequence similarity nor related three-dimensional structures. Plant 1,3-1,4-β-glucanases are essentially expressed during germination and facilitate the action of amylolytic enzymes on starch by breaking down the 1,3-1,4-β-glucan rich amylaceous cell walls (*4*). Barley 1,3-1,4-β-glucanase and 1,3-β-glucanase, a protein involved in the defense against pathogenic fungi, show a high sequence homology and similar three-dimensional α/β-barrel structure, pointing toward a common ancestor for both enzymes (*5*). The function of bacterial 1,3-1,4-β-glucanases is less well defined. The fact that they usually are extracellular enzymes seems to indicate an involvement in the degradation of polysaccharides that can be present in the natural enviroment of bacteria and that can be used as an energy source by these microorganisms. Genes encoding bacterial 1,3-1,4-β-glucanases have been cloned and sequenced from different *Bacillus* species, *Fibrobacter succinogenes*, *Ruminococcus flavofaciens*, and *Clostridium thermocellum* (*6*). Together with bacterial 1,3-β-glucanases ("laminarinases"), all bacterial 1,3-1,4-β-glucanases share a high degree of sequence similarity, and have been classified as members of family 16 of glycosyl hydrolases (*7*, *8*). They are highly homologous proteins, with molecular masses in the range of 25−30 kDa, are active in a wide pH range, have a basic p*I* (8−9), and are quite thermostable compared to the plant isozymes. As shown for the *Bacillus licheniformis* enzyme, bacterial 1,3-1,4-β-glucanases are "retaining" glycosidases leading to retention of configuration of the cleaved glycosidic bond during the hydrolysis of barley β-glucan (*3*).

Important progress on the structure−function relationships in *Bacillus* 1,3-1,4-β-glucanases includes identification of the catalytic residues by site-directed mutagenesis and chemical modification with active-site directed inhibitors. The use of epoxyalkyl oligosaccharides as suicide inhibitors of the *B. amyloliquefaciens* enzyme (*9*) has allowed the identification of Glu105 as the essential nucleophile. The systematic mutational analysis of the *B. licheniformis* enzyme identified Glu134 (the equivalent to Glu105 in *B. amyloliquefaciens*) and Glu138 as the catalytic nucleophile and the general acid−base catalyst, respectively (*10*, *11*). The same residues were also identified in the *B. macerans* isozyme (*12*). The three-dimensional structures of the wt *B. macerans* (*12*) and *B. licheniformis* (*13*) enzymes have been solved, as well as several hybrids of *B. amyloliquefaciens* and *B. macerans* (*14*). They show nearly identical jelly roll β-sandwich structures, with a carbohydrate-binding cleft

† This work was supported by Grant BIO94-0912-C02-02 from the Comisión Interministerial de Ciencia y Tecnología, Madrid, Spain.

* Author to whom correspondence should be addressed. FAX: +34-3-205 62 66. E-mail: aplan@iqs.url.es.

⊗ Abstract published in *Advance ACS Abstracts,* October 15, 1997.

[1] Abbreviations: 1,3-1,4-β-glucanase, 1,3-1,4-β-D-glucan 4-glucanohydrolase; DTNB, 5,5′-dithiobis-2-nitrobenzoic acid; EAC, 1-ethyl-3[3-(dimethylamino)propyl]carbodiimide; HEPES, *N*-(2-hydroxyethyl)-piperazine-*N*-2-ethanesulfonic acid; MES, 2-(*N*-morpholino)ethanesulfonic acid; TAPS, *N*-tris[hydroxymethyl]methyl-3-aminopropanesulfonic acid; wt, wild type.

S0006-2960(97)01134-3 CCC: $14.00

Chart 1

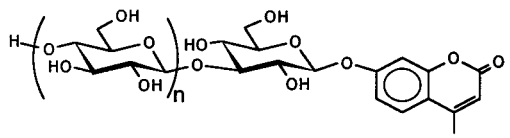

1a n=0 G-MU
1b n=1 G3G-MU
1c n=2 G4G3G-MU
1d n=3 G4G4G3G-MU
1e n=4 G4G4G4G3G-MU

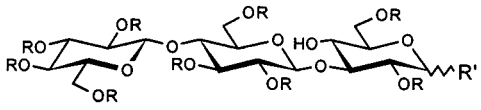

3 R = H R' = OH **5** R = Ac R' = β-OMe
4 R = Ac R' = α-Br **2a** R = H R' = β-OMe

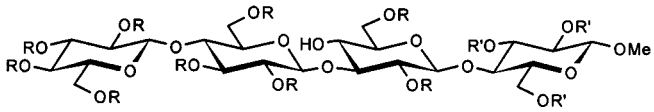

6 R = Ac R' = Bn **2b** R = H R' = H
7 R = H R' = Bn

located on the concave face of a β-sheet formed of consecutive antiparallel β-strands. Quite similar three-dimensional structures have been described for the catalytic core of cellobiohydrolase I from *Trichoderma reesei* (family 7, refs 15 and 16) and a *B. circulans* xylanase (family 11, ref 17) as well as some plant legume lectins.

In spite of the important amount of structural information derived from both protein crystallography and site-directed mutagenesis, no detailed kinetic studies aimed at a better understanding of both substrate specificity and catalysis at the molecular level have been reported so far. Kinetics with the natural polymeric substrates provide little information, and no simple models can be derived since each initial polysaccharide molecule is cleaved several times by the enzyme. Identification of key carbohydrate−protein interactions, and measurement of discrete contributions to binding and catalysis require the use of low molecular weight substrates and inhibitors. Toward this goal, the 1,3-1,4-β-D-glucan oligosaccharides **1a**−**e** (Chart 1) carrying an aglyconic chromophoric marker have been recently prepared in our group (*18*, *19*). Here we describe the application of these specific 1,3-1,4-β-glucanase substrates in the subsite mapping of the extended binding cleft of *B. licheniformis* 1,3-1,4-β-glucanase and in pH−activity dependence studies.

MATERIALS AND METHODS

Substrates. The 4-methylumbelliferyl glycosides of glucopyranose (**1a**, G-MU), 3-*O*-β-D-glucopyranosyl-β-D-glucopyranose (**1b**, G3G-MU), 3-*O*-β-cellobiosyl-β-D-glucopyranose (**1c**, G4G3G-MU), 3-*O*-β-cellotriosyl-β-D-glucopyranose (**1d**, G4G4G3G-MU), and 3-*O*-β-cellotetraosyl-β-D-glucopyranose (**1e**, G4G4G4G3G-MU) were synthesized as reported previously (*18*).

The methylglycosides **2a** (G4G3G-βOMe) and **2b** (G4G3G4G-βOMe) were prepared from barley β-glucan according to the following procedures. Barley β-glucan (Sigma) was degraded by 1,3-1,4-β-glucanase from *Bacillus licheniformis* down to a tri- and tetrasaccharides (*3*). The trisaccharide **3** (3-*O*-β-cellobiosyl-β-D-glucopyranose) was acetylated in a mixture of Ac_2O/pyridine, and the anomeric position was activated by formation of the bromoderivative as reported elsewhere (*19*). The α-glycosyl bromide (**4**) was then transformed into the target methylglycosides as follows (yields have not been optimized).

*Methyl3-O-β-Cellobiosyl-β-D-glucopyranoside(**2a**,G4G3G-βOMe).* A 1.23 g (1.25 mmol) amount of the α-glycosyl bromide **4** in 2 mL of CH_2Cl_2 was added to a stirred mixture of 0.54 mL (13.5 mmol) of MeOH, 403 mg (1.12 mmol) of $HgBr_2$, 283 mg (1.12 mmol) of $Hg(CN)_2$, 2 g of powdered molecular sieves (4 Å), and 1 mL of CH_2Cl_2 under Ar atmosphere. After being stirred at room temperature for 17 h, the reaction mixture was filtered through Celite, washed with a saturated $NaHCO_3$ solution until neutral, followed by water, and dried over magnesium sulfate. Evaporation of the solvent gave a raw material that was purified by flash chromatography on silica gel ($CHCl_3$/AcOEt 3:2) to yield 710 mg (69%) of **5**: $[\alpha]_D^{20}$ −0.2° (*c* 0.509, $CHCl_3$), ^{1}H-NMR (300 MHz, $CDCl_3$): 1.98−2.14 (10s, 30H), 3.47 (s, 3H), 3.54−3.68 (m, 3H), 3.77 (dd, J = 8.0 Hz, 1H), 3.82 (dd, J = 8.0 Hz, 1H), 4.00−4.24 (m, 4H), 4.32−4.44 (m, 2H), 4.29 (d, J = 7.8 Hz, 1H), 4.47 (d, J = 8.1 Hz, 1H), 4.55 (d, J = 7.8 Hz, 1H), 4.80−5.18 (m). ^{13}C-NMR (75 MHz, $CDCl_3$): 20.3−21.0, 56.6, 61.5, 62.1, 62.2, 67.8, 68.3, 71.1, 71.6, 71.8, 72.0, 72.6, 72.8, 72.9, 76.3, 79.1, 100.8, 100.9, 101.5, 168.9−170.7. A 583 mg (0.62 mmol) amount of compound **5** was dissolved in 6 mL of 20 mM sodium methoxide in MeOH, and the solution was stirred at 30 °C for 17 h. Excess Amberlite IR-120(H^+) was added, the mixture stirred for 10 min and filtered. Evaporation of the solvent yielded 315 mg (90%) of **2a**: mp (recrystallized from H_2O/EtOH) 108−110 °C (dec); $[\alpha]_D^{20}$ −0.2 (*c* 0.509, H_2O). Anal. Calcd for $C_{19}H_{34}O_{16}$: C, 44.0; H, 6.61. Found: C, 43.9; H, 6.89. ^{1}H-NMR (300 MHz, D_2O): 3.58 (s, 3H), 3.30−4.00 (m), 4.41 (d, J = 8.1 Hz, 1H), 4.51 (d, J = 7.8 Hz, 1H), 4.76 (d, J = 7.8 Hz, 1H). ^{13}C-NMR (75 MHz, D_2O): 60.1, 62.9, 63.4, 63.6, 71.0, 72.3, 75.6, 76.0, 76.1, 77.0, 77.7, 78.4, 78.9, 81.4, 87.4, 105.4, 105.8.

*Methyl O-β-D-Glucopyranosyl-(1 → 4)-O-β-D-glucopyranosyl-(1 → 3)-O-β-D-glucopyranosyl-(1 → 4)-β-D-glucopyranoside (**2b**, G4G3G4G-βOMe)*

(a) Glycosidation. A mixture composed of 2.58 g (5.56 mmol) of methyl 2,3,6-tri-*O*-benzyl-β-D-glucopyranoside (*20*), 1.04 g (2.88 mmol) of $HgBr_2$, 728 mg (2.88 mmol) of $Hg(CN)_2$, 3 g of powdered molecular sieves (4 Å), and 10 mL of CH_2Cl_2 was stirred under Ar at room temperature for 1 h. A solution of the α-glycosyl bromide **4** in 5 mL of CH_2Cl_2 was then added, and the mixture was stirred at room temperature for 21 h. After being filtered through Celite, the reaction mixture was washed with saturated $NaHCO_3$ solution followed by water and dried over magnesium sulfate. Evaporation of the solvent yielded 5.3 g of raw material that was chromatographed on silica gel (toluene/AcOEt 7:1, 5:1). Eluted first were unreacted starting materials (3.8 g), and second was **6** that required a further chromatographic purification on a Lichroprep RP-18 Column (Merck) (CH_3CN/H_2O 1:2 → 1.5:1) (final yield 14%, 920 mg): $[\alpha]_D^{20}$ −0.1° (*c* 0.400, $CHCl_3$). Anal. Calcd for $C_{66}H_{82}O_{31}$: C,

57.8; H, 6.03. Found: C, 57.8; H, 6.29. ^{1}H-NMR (300 MHz, $CDCl_3$): 1.94−2.12 (10s, 30H), 3.55 (s, 3H), 3.20−5.14 (m), 7.25−7.39 (m, 15H). ^{13}C-NMR (75 MHz, $CDCl_3$): 20.3−20.9, 57.0, 61.5, 61.8, 62.4, 67.6, 67.7, 67.9, 71.0, 71.6, 72.0, 72.6, 72.8, 73.1, 73.7, 74.7, 75.0, 76.4, 79.1, 81.6, 82.5, 100.0, 100.8, 100.9, 104.6, 127.2−128.5, 138, 138.5, 139, 168.6−170.7.

(b) Removal of Protecting Groups (Acetyl + Benzyl). A solution of 500 mg (0.36 mmol) of **6** in 6.5 mL of 20 mM sodium methoxide in MeOH was stirred at 30 °C for 16 h. The reaction mixture was neutralized with excess Amberlite IR-120(H^+), and the resin was removed by filtration. Evaporation of the solvent yielded 291 mg (84%) of **7**. ^{1}H-NMR (300 MHz, d_6-DMSO + D_2O): 3.00−3.95 (m), 3.51 (s, 3H), 4.31 (d, J = 7.8 Hz), 4.44 (d, J = 7.8 Hz, 1H), 4.48 (d, J = 8.1 Hz, 1H), 4.51 (d, J = 8.1 Hz, 1H), 4.57 (d, 11.1 Hz, 1H), 4.63 (d, J = 12.3 Hz, 1H), 4.64 (d, J = 11.7 Hz, 1H), 4.70 (d, J = 11.1 Hz, 1H), 4.81 (d, J = 11.7 Hz, 1H), 5.01 (d, J = 11.1 Hz, 1H), 7.31−7.43 (sc, 15H).

A 206 mg (0.27 mmol) amount of compound **7** in 2.5 mL of H_2O/EtOH/THF 2:2:1 (v/v) was added to a pre-hydrogenated suspension of 140 mg of Pd-C (10%) in 2 mL of the same solvent. After being stirred at 30 °C under H_2 atmosphere for 28 h, the mixture was filtered through Celite. Evaporation of the solvent gave 175 mg (93%) of **2b**: $[\alpha]_D^{20}$ −0.1 (*c* 0.306, H_2O); ^{1}H-NMR (300 MHz, D_2O): 3.56 (s, 3H), 3.25−4.00 (m), 4.38 (d, J = 8.1 Hz, 1H), 4.48 (d, J = 8.1 Hz, 1H), 4.51 (d, J = 8.1 Hz, 1H), 4.76 (d, J = 7.8 Hz, 1H). ^{13}C-NMR (75 MHz, D_2O)**:** 60.1, 62.9, 63.4, 70.8, 72.3, 75.7, 76.0, 76.1, 77.0, 77.2, 77.6, 77.7, 78.3, 78.4, 78.8, 81.5, 86.7, 105.2, 105.4, 105.9.

Enzyme. 1,3-1,4-β-Glucanase was obtained from recombinant *Escherichia coli* HB101 harboring a *B. licheniformis* β-glucanase expression plasmid as previously reported (*10*). The enzyme was purified from the culture supernatant according to Planas *et al.* (*21*) with an additional purification step by FPLC on an ion-exchange TSK CM-3SW column in 5 mM acetate buffer pH 5.6 and eluted with a linear gradient 0−0.4 M NaCl in the same buffer. Purity was higher than 95% as judged by SDS-polyacrylamide gel electrophoresis according to Laemmli (*22*). Enzyme concentration in all runs was determined by UV spectrophotometry using ϵ_{280nm} 14.5 cm^{-1} mL mg^{-1} (3.55×10^5 M^{-1} cm^{-1}) (*23*).

HPLC and ^{1}H-NMR Monitoring. The specificity of cleavage and time course of the enzymatic hydrolysis of the 4-methylumbelliferyl glycosides were analyzed by monitoring the reactions of **1a**−**e** (4 mM) in citrate−phosphate buffer (6.5 mM citric acid, 87 mM Na_2HPO_4) pH 7.2, 0.1 mM $CaCl_2$ and 0.25 μM enzyme for reactions with substrates **1b**−**e**, 1 μM for reactions with **1a**, at 55 °C. Samples were withdrawn at regular time intervals (50 μL), diluted to 500 μL in H_2O/MeOH 1:1, and analyzed by HPLC in a Novapack C-18 column (Waters, 3.9 × 140 mm, 4 μm particles) using a 10 μL injection loop and a UV detector at 316 nm. Elution was 0−17 min MeOH/H_2O 14:86 (v/v), 17−25 min linear gradient up to MeOH/H_2O 60:40, at a flow rate of 1 mL min^{-1} at 30 °C. The endpoints of the enzymatic hydrolyses of **1a**−**e**, as well as the monitoring of the reactions with the methylglycosides **2a** and **2b** (4 mM, same conditions as above but using 8.2 nM enzyme for **2b** and 0.5 μM enzyme for **2a**), were analyzed in an Aminex HPX-42A column (Bio-Rad) eluted with H_2O at a flow rate of 0.6 mL min^{-1} at 85 °C. The free oligosaccharide products were detected with a refractive index detector.

^{1}H-NMR monitoring of the enzymatic hydrolysis of **1d** was done in D_2O at 28 °C in 100 mM sodium phosphate−disodium phosphate buffer (the salts were previously freeze-dried 3 times from 99.8% D_2O and one more time from 99.95% D_2O), and the pD adjusted to 7.3 with 1 N NaOD/D_2O. Substrate concentration was 7.2 mM, and the enzyme concentration was adjusted to 7.2 μM to obtain hydrolysis rates faster than mutarotation of the newly formed reducing ends. ^{1}H-NMR spectra were recorded on a Varian VXR 500 spectrometer every 5 min after 20 min from mixing the enzyme and the buffered substrate solution in the NMR tube. The reaction was monitored for a total time of 80 min. The residual HDO signal was minimized using inversion-recovery (time between pulses 4.5 s). Integration of the resonance signals was done after baseline correction with a third-order polynomial function.

Enzyme Kinetics

*(a) Kinetics with Barley β-Glucan and the Methyl Glycoside **2b**.* Enzyme-catalyzed hydrolyses were performed by incubating the appropriate concentration of substrate (0.2−8 mg mL^{-1} for barley β-glucan, 0.5−7 mM for the methylglycoside **2b**) in citrate−phosphate buffer (6.5 mM citric acid, 87 mM Na_2HPO_4), pH 7.2, 0.1 mM $CaCl_2$ in a thermostated bath at 55 °C. After a 5 min pre-incubation, reactions were initiated by adding the enzyme to a final concentration of 50 nM to 1 μM. Initial rates were obtained by determining the net release of reducing sugars at one-minute intervals for a total time of 5−8 min by the Somogyi−Nelson method (*24*, *25*). Reducing power was expressed as equivalent trisaccharide 3-*O*-β-cellobiosyl-D-glucose concentration, and the rates were given in mM trisaccharide per second.

(b) pH Profile with Barley β-Glucan. Reactions were done in citrate−phosphate buffer (11 mM citric acid, 11 mM KH_2PO_4) for the pH range 4.3−7.5, and in 11 mM TAPS buffer for the pH range 7.5−10, adjusting the pH to the required value with KOH, 0.1 mM $CaCl_2$, and keeping the ionic strength constant at 0.1 M with added KCl. A saturating barley β-glucan concentration (6 mg mL^{-1}) was used in all runs to evaluate the pH dependence of V_{max}. After a 5 min pre-incubation at 55 °C, the enzyme was added to a final concentration of 20 nM. Initial rates were determined by the Somogyi−Nelson method as described above.

*(c) Kinetics with the 4-Methylumbelliferyl Glycosides **1a**−**e**.* All kinetics were performed by following changes in UV absorbance due to the release of 4-methylumbelliferone using matched 1-cm path length cells in a Perkin-Elmer λ2 spectrophotometer equipped with a circulating water bath which maintained the cells at 53 °C. Rates of the enzyme-catalyzed hydrolyses were determined by incubating the substrate at the appropriate concentration in citrate−phosphate buffer (6.5 mM citric acid, 87 mM Na_2HPO_4), pH 7.2, 0.1 mM $CaCl_2$ for 5 min in the thermostated cell holder. Reactions were initiated by the addition of the enzyme and monitoring the absorbance change at λ 365 nm ($\Delta\epsilon$ = 5440 M^{-1} cm^{-1}, see below).

The concentration of stock solutions of **1a**−**e** were determined by UV spectrophotometry using the molar extinction coefficient reported for 4-methylumbelliferyl glycosides ϵ_{316} = 13 600 M^{-1} cm^{-1} (*26*). The molar extinction coefficients at the working wavelengths (λ_{355nm} for kinetics

at pH < 7, λ_{365nm} for kinetics at pH ≥ 7) were $\epsilon_{355} = 265$ M^{-1} cm^{-1} and $\epsilon_{365} = 177$ M^{-1} cm^{-1} and were pH independent. The pH-dependent molar extinction coefficients of 4-methylumbelliferone (MU-OH) at 355 and 365 nm were accurately measured at the conditions used for the kinetic assays (buffer concentration and ionic strength) using a stock solution of MU-OH (recrystallized three times from AcOH) in H_2O [concentration determined in 100 mM TAPS pH 10.3, $\epsilon_{360} = 16\,720$ M^{-1} cm^{-1} (*27*)] diluted in the appropriate buffer, the pH adjusted at 53 °C. Values of ϵ_{355} and ϵ_{365} at different pH values were fitted by nonlinear regression to the equation

$$\epsilon_{MU-OH,\lambda} = (\epsilon_{MH,\lambda} + \epsilon_{M^-,\lambda} \times 10^{(pH-pK_a)})/(1 + 10^{(pH-pK_a)})$$

where MH and M^- are the unionized and ionized forms of 4-methylumbelliferone, respectively, and $\epsilon_{MU-OH,\lambda}$ is the measured molar extinction coefficient at each λ. The adjusted parameters were $\epsilon_{MH,355} = 824$ M^{-1} cm^{-1}, $\epsilon_{M^-,355} = 15810$ M^{-1} cm^{-1}, $\epsilon_{MH,365} = 86$ M^{-1} cm^{-1}, $\epsilon_{M^-,365} = 15810$ M^{-1} cm^{-1}, and $pK_a = 7.53$ for the ionization of MH, in 11 mM citrate−11 mM phosphate buffer, constant ionic strength of 0.1 M, 53 °C.

*(d) pH Dependence with the 4-Methylumbelliferyl Trisaccharide **1c**.* The kinetic parameters as a function of the pH for the enzyme-catalyzed hydrolysis of **1c** were determined as in c in citrate−phosphate buffer (11 mM citric acid, 11 mM KH_2PO_4) adjusting the pH at 53 °C to the required value with KOH, 0.1 mM $CaCl_2$, and keeping constant the ionic strength to 0.1 M with added KCl. The release of 4-methylumbelliferone was monitored at λ_{355nm} for reactions at pH < 7 and at λ_{365nm} for reactions at pH ≥ 7, using the appropriate $\Delta\epsilon_\lambda$ ($= \epsilon_{MU-OH,\lambda} - \epsilon_{\mathbf{1c},\lambda}$) at each pH.

Enzyme Inactivation by EAC

Chemical modification of carboxylic groups of 1,3-1,4-β-glucanase was accomplished by reaction with the water-soluble carbodiimide EAC, in the absence of an added nucleophile. The enzyme (0.7 μM) was treated with EAC (5−75 mM, final concentration) in 50 mM MES, pH 6.0, and incubated at 25 °C for 60−90 min. Aliquots were withdrawn at indicated times, the reaction was quenched with sodium acetate, pH 4.7 (final concentration 100 mM), and the residual enzyme activity was determined at pH 7.2 with barley β-glucan (4 mg mL^{-1}) as in Enzyme Kinetics, a above, or with the pentasaccharide substrate **2e** (2 mM) as in c. In a parallel experiment, the chemical modification of the enzyme (0.4 μM) with EAC (30 mM) was done in the presence of cellobiose (5−45 mM). For the pH-dependence of EAC inactivation, the enzyme (10 μM) was incubated with 30 mM EAC in MES (25 mM)/HEPES (25 mM)/4-hydroxy-1-methylpiperidine (25 mM) ternary (constant ionic strength) buffer (*28*) at 25 °C, pH ranging from 4 to 8.5, for a total time of 2 h. At appropriate time intervals, 15 μL of the reaction mixture was added to 40 μL of 140 mM sodium acetate, pH 4.7. Residual activity was determined with substrate **2e** (2 mM) at pH 7.2, 53 °C as described above.

RESULTS

Substrates. The criteria for designing the substrates were (a) a basic core structure G3G-X according to the requirements of natural polysaccharide substrates (barley β-glucan and lichenan) to be hydrolyzed by the enzyme, *i.e.* cleavage of glycosidic bonds on a 3-*O*-substituted glucopyranose units; (b) single scissile glycosidic bond to simplify interpretation of kinetic data; (c) release of a chromophoric aglycon upon enzymatic hydrolysis for easy monitoring of the reaction course by continuous UV or fluorescence spectroscopy. The choice of a 4-methylumbelliferyl aglycon as a chromophoric glucopyranose mimic was based on the extensive kinetic studies of cellulases using 4-methylumbelliferyl cellooligosaccharides (*26*, *29*, *30*). The preparation of compounds **1a**−**e** has been recently reported by our group both by total chemical synthesis (*18*) and by a chemoenzymatic approach (*19*).

Specificity of Hydrolysis and Stereochemical Course. HPLC monitoring of the enzymatic reaction of **1a**−**e** showed that all glycosides are accepted as substrates by the *B. licheniformis* 1,3-1,4-β-glucanase. Cleavage occurs regiospecifically on the glycosidic bond linking the glyconic moiety and the chromophoric aglycon, and no further enzymatic cleavage of the released reducing sugar was detected. The results are in agreement with the known substrate specificity of the enzyme on its natural polymeric substrates and in accordance with the design of these low molecular weight substrates.

^{1}H-NMR monitoring of the enzymatic cleavage of the tetrasaccharide **1d** showed the reaction to proceed with the same stereoespecificity observed in the depolymerization of barley 1,3-1,4-β-glucan, leading to net retention of the anomeric configuration of the cleaved glycosidic bond. Figure 1 shows the main changes in the anomeric region of the ^{1}H-NMR spectrum during the enzymatic cleavage. As main features, a doublet at 4.68 ppm ($J = 8$ Hz) develops during the first minutes of the enzymatic reaction at the same rate at which the glycoside is cleaved, proving the β-configuration on H-1A of the newly formed reducing sugar. Under the conditions chosen in the experiment significant mutarotation is observed only after 20 min of reaction, slowing down the apparent formation of reducing ends with β-configuration and leading to the expected 6:4 β/α ratio in the thermally equilibrated mixture of anomers.

Kinetic Parameters. Steady state kinetics of hydrolysis with substrates **1a**−**e** were performed in citrate−phosphate buffer at pH 7.3, 53 °C, conditions of maximum activity on the natural substrate β-glucan. Initial velocities (<3% conversion) at different substrate concentrations were determined by monitoring the release of 4-methylumbelliferone at 365 nm ($\Delta\epsilon = 5440$ M^{-1} cm^{-1}). The monosaccharide **1a** is a poor substrate. Long incubation times and high enzyme concentration were required to allow detection of products (e.g., 1.5 μM enzyme, less than 0.1% conversion of substrate after 40 min), and no saturation kinetics were observed up to 10 mM. For the oligosaccharides **1b**−**e** the curve v_o *vs* [S] reaches a maximum and decreases at higher substrate concentration (Figure 2). The data were fitted to eq 1, which corresponds to an uncompetitive substrate inhibition model.

$$v_0 = \frac{k_{cat}[E_0][S]}{K_M + [S] + ([S]^2/K_I)} \quad (1)$$

A clearly biphasic Hill plot, $\log[v/(V - v)]$ *vs* log[S], shown in Figure 2 (inset) is consistent with this inhibition scheme, where a second molecule of substrate is able to bind into the extended binding site with formation of unproductive ternary complexes (ES_2), producing a downward curvature at high substrate concentration with the slope becoming

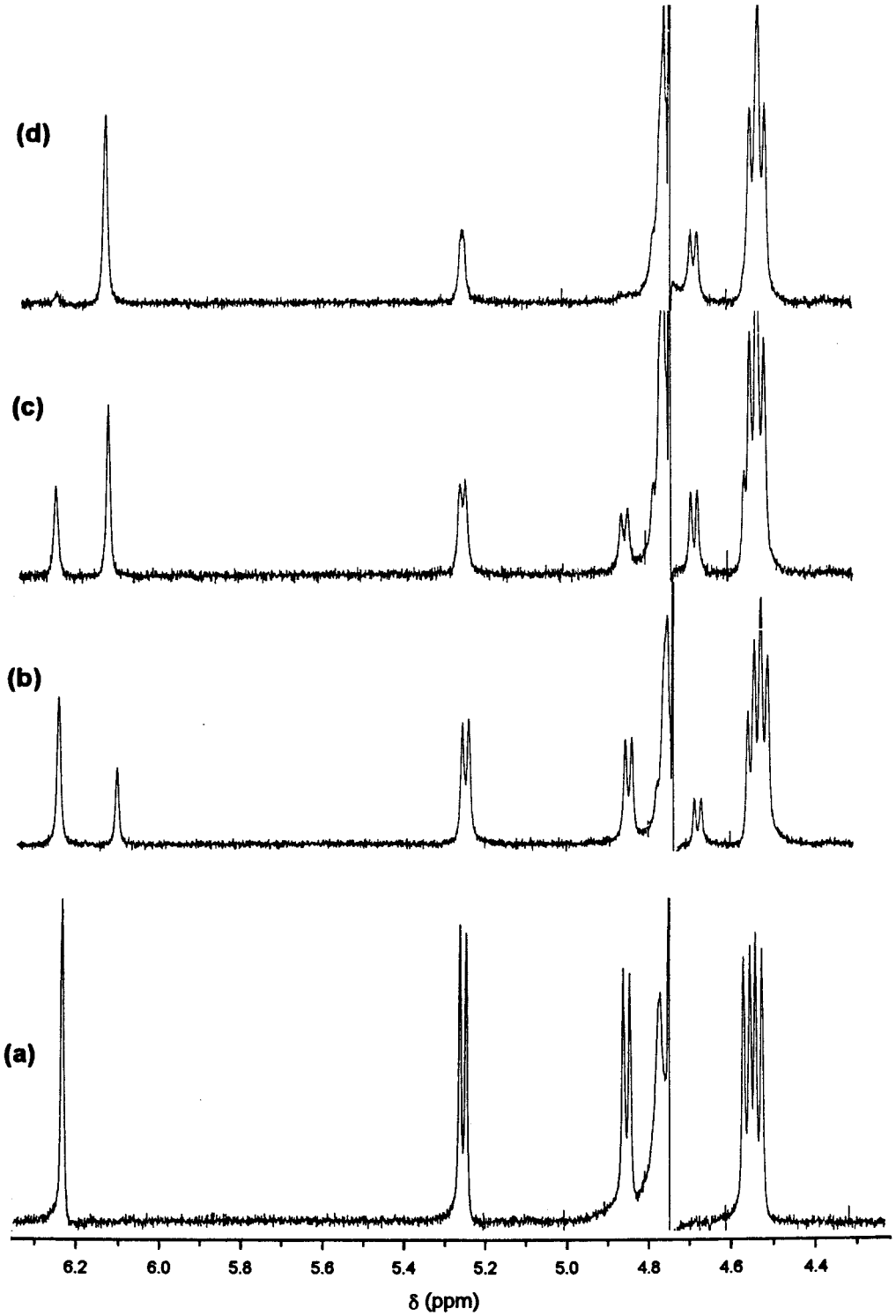

FIGURE 1: ^{1}H-NMR spectra of the anomeric region for the 1,3-1,4-β-glucanase-catalyzed hydrolysis of **1d**. The reaction was done in D_2O at 28 °C in 100 mM phosphate buffer, pD 7.3, [E] = 7.2 μM, [S] = 7.2 mM. (a) Substrate **1d**. (b−d) After 20, 40, and 80 min, δ in ppm: 6.25, H-3′ of **1c**, 6.10, H-3′ of 4-methylumbelliferone, 5.25, H-1A of **1d** + H-1A (α-anomer) of the hydrolysis product, and 4.86, H-1B of **1d**; and 4.68 (J = 8 Hz), H-1A (β-anomer) of the hydrolysis product. The initial rates of formation of the signals at δ 4.68 and 6.10 ppm (formation of the β-anomer of the hydrolysis product and release of 4-methylumbelliferone, respectively) are equal, proving that the reaction proceeds with retention of configuration.

negative ($h = -1$). Kinetic parameters for compounds **1a**−**e** are summarized in Table 1.

The dependence of k_{cat} and K_M as a function of the glyconic chain length reaches a plateau between the tetrasaccharide **1d** and the pentasacharide **1e**, indicating that the addition of a fifth glucopyranose unit on the reducing end of **1d** has little or no effect either in apparent binding or catalysis. Since all substrates exhibit the same hydrolysis pattern, the kinetic results are in agreement with an extended binding site cleft composed of four subsites for glucopyranose units on the non-reducing end from the scissile glycosidic bond (subsites −I to −IV).[2]

Subsite Mapping. Since the enzyme is an heterodepolymerase hydrolyzing a single glycosidic bond of the reported oligosaccharide substrates, conventional subsite mapping based on bond-cleavage frequencies on homopolymeric substrates as a function of the chain length (*31*, *32*) cannot be applied. The observed uncompetitive substrate inhibition

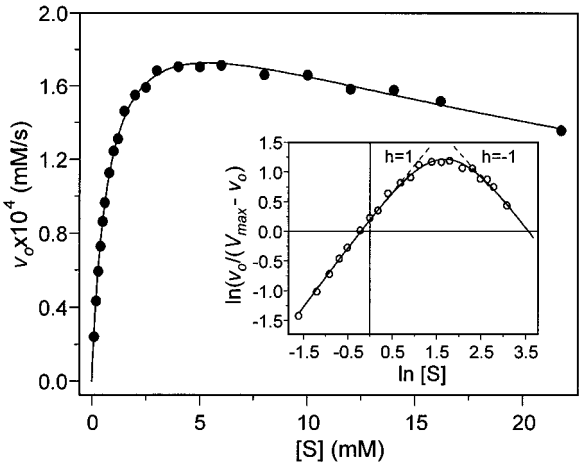

FIGURE 2: Steady-state kinetics for the enzyme-catalyzed hydrolysis of **1d**. Inset: Hill plot. Conditions: 6.5 mM citrate−87 mM phosphate buffer, pH 7.2, 53 °C, 0.1 mM $CaCl_2$, [E] = 25.2 nM. Kinetic parameters are given in Table 1.

behavior for **1b**−**e** provides strong evidence for multiple binding modes, only one leading to a productive complex followed by specific hydrolysis at a single glycosidic bond. As deduced in the Appendix, the experimental k_{cat} and K_M values are dependent on productive and unproductive complexes, and the lack of other substrates to map the reducing end of the binding cleft precludes the application of a formal subsite mapping calculation to estimate binding energies. However, the contribution of single subsites to transition state stabilization can be calculated from the second-order rate constants k_{cat}/K_M, and can be expressed by the difference in transition state activation energy between two substrates differing in one glucopyranose unit according to

$$\Delta G^{\ddagger}_{subsite} = \Delta G^{\ddagger}_{n+1} - \Delta G^{\ddagger}_{n} = -RT \ln \frac{(k_{cat}/K_M)_{n+1}}{(k_{cat}/K_M)_n} \quad (2)$$

The values of $\Delta G^{\ddagger}_{n+1}$ calculated from the kinetic data for the hydrolysis of the 4-methylumbelliferyl glycosides **1a**−**e** are summarized in Table 2. Binding of 4-*O*-substituted glucopyranose units to subsites −II to −IV have a stabilizing effect on the enzyme−carbohydrate transition state complex, with a larger contribution of subsite −III (−3.5 kcal/mol).

Kinetics with β-Methyl Glycosides. HPLC and ^{1}H-NMR analysis showed unambiguously that **2a** (G4G3G-βOMe) is not a substrate of *B. licheniformis* 1,3-1,4-β-glucanase, since no traces of possible products were detected after 15 h of incubation of a 5 mM solution of this trisaccharide with 0.5 μM enzyme under conditions of maximum activity (55 °C, pH 7.2). It indeed behaves as a competitive inhibitor of the enzyme-catalyzed hydrolysis of the 4-MU trisaccharide **1c** with an inhibition constant of 2.0 ± 0.5 mM. For the inhibition experiments, the range of substrate concentration was chosen below K_M [0.33 mM ≤ [S] ≤ 1 mM, K_M (**1c**) = 2.7 mM] and far below K_I (**1c**) = 38 mM (Table 1) to avoid complex behavior arising from substrate inhibition.

On the other hand, the tetrasaccharide **2b** (G4G3G4G-βOMe) is efficiently cleaved by the enzyme yielding the expected trisaccharide **3** and methyl β-D-glucopyranoside, the reaction being essentially complete after 5 min under the same experimental conditions that do not yield any product for **2a**. No transglycosidation products were detected by either HPLC or ^{1}H-NMR monitoring. The kinetic parameters for the hydrolysis of **2b** were determined by measurement of the increase in reducing power associated with the enzymatic cleavage according to the method of Somogyi and Nelson. The experimental data were fit to a rectangular hyperbole with $K_M = 2.6 \pm 1$ mM and $k_{cat} = 78 \pm 14$ s^{-1} ($k_{cat}/K_M = 30\,000 \pm 17\,000$ M^{-1} s^{-1}). Although no apparent substrate inhibition was observed in the range of concentrations used, such a model (as observed for the 4-methylumbelliferyl glycosides **1b**−**e**) cannot be ruled out because the accuracy of the data is rather limited due to the inherent experimental error associated with reducing power measurements.

pH Dependence of the Kinetic Parameters. The steady-state values of k_{cat}, K_M, and k_{cat}/K_M for the 1,3-1,4-β-glucanase-catalyzed reaction of **1c** were measured over a pH range of 4−9 in citrate−phosphate buffer and constant ionic strength (100 mM) with added KCl. Other buffers such as HEPES or the ternary buffer AcOH/ACES/DEA (*28*) showed a pronounced effect on K_M values. HEPES behaves as an inhibitor changing the K_M value for **1c** from 3.3 mM in 50 mM buffer to 7.0 mM in 200 mM buffer at pH 7.2. The pH profiles of the catalytic parameters are plotted in Figure 3. The pH dependence of k_{cat} follows a single ionization curve; k_{cat} values at pH lower than 4.5 could not be determined because of the large increase of K_M at acidic pH. The plot of k_{cat}/K_M against pH shows a bell-shaped curve corresponding to a double-ionization process. The kinetic pK_a and limiting k_{cat} and k_{cat}/K_M values were obtained from nonlinear regression fitting of the data to eqs 3 (k_{cat}) and 4 (k_{cat}/K_M), where $(k_{cat})_{lim}$, $(k_{cat}/K_M)_{lim}$, pK_a, pK_{a1}, and pK_{a2} are the adjustable parameters. Results are summarized in Table 3.

$$k_{cat} = \frac{(k_{cat})_{lim}}{1 + 10^{pH-pK_a}} \quad (3)$$

Kinetic pK_a values were also determined for barley β-glucan

$$k_{cat}/K_M = \frac{(k_{cat}/K_M)_{lim}}{1 + 10^{pK_{a1}-pH} + 10^{pH-pK_{a2}}} \quad (4)$$

as substrate in citrate−phosphate buffer for reactions in the pH range 4−7.5 and in TAPS buffer (which does not inhibit the enzyme) from 7.5 to 10 (constant ionic strength of 100 mM with added KCl). Only data on k_{cat} (Figure 3) could be measured accurately since K_M values are subject to large errors due to the heterogeneity of the natural polysaccharide substrate (*21*). Fitting the data to eq 5

$$k_{cat} = \frac{(k_{cat})_{lim}}{1 + 10^{pK_{a1}-pH} + 10^{pH-pK_{a2}}} \quad (5)$$

gave the kinetic pK_{a1}, pK_{a2}, and $(k_{cat})_{lim}$ values (Table 3).

pH Dependence of the Chemical Inactivation by EAC

The ionization of essential carboxyl groups involved in the mechanistic pathway was investigated by chemical modification using the water-soluble carbodiimide EAC. This reagent is specific for the protonated carboxyl form and thus reacts in a pH-dependent manner (*33*). Incubation of 1,3-

[2] Subsites are numbered −I to −IV on the non-reducing end of the scissile glycosidic bond. According to the 3D structure determined by X-ray crystallgraphy (*13*), the binding site cleft also contains two or three glucopyranose binding subsites on the reducing end, +I to +III from the position of the glycosidic bond being hydrolyzed.

Table 1: Michaelis−Menten Parameters of *B. licheniformis* 1,3-1,4-β-Glucanase with Substrates **1a**−**e** and the β-Methyl Glycosides **2a**,**b**

substrate	K_M (mM)	k_{cat} (s^{-1})	K_I (mM)	k_{cat}/K_M (M^{-1} s^{-1})
1a G-MU[a]				0.348 ± 0.008
1b G3G-MU	16.8 ± 2.2	0.139 ± 0.012	57.2 ± 11.5	8.27 ± 1.80
1c G4G3G-MU	2.69 ± 0.06	4.58 ± 0.06	37.8 ± 1.5	1700 ± 60
1d G4G4G3G-MU	0.79 ± 0.02	8.86 ± 0.10	36.4 ± 1.8	11 200 ± 500
1e G4G4G4G3G-MU	0.66 ± 0.03	8.78 ± 0.20	29.3 ± 4.9	13 300 ± 900
2a G4G3G-βOMe	2.0 ± 0.5 (K_I)[b]			
2b G4G3G4G-βOMe	2.6 ± 1.0	78 ± 14		30 000 ± 17 000

[a] MU, 4-methylumbelliferyl. Conditions: 6.5 mM citrate−87 mM phosphate buffer, pH 7.2, 53 °C, 0.1 mM $CaCl_2$, [E] = 25−150 nM, [S], **1a**, 1−10 mM, **1b**, 1−51 mM, **1c**, 0.1−24 mM; **1d**, 0.1−22 mM; **1e**, 0.1−6 mM. [b] Inhibition constant for **2a** using **1c** as substrate. [E] = 45 nM, [**1c**] = 0.3−1 mM, [**2a**] = 0−10 mM. Reactions with **1a**−**c** were monitored by UV spectrophotometry, and reactions with **2b** were monitored by measuring the increase of reducing power as described under Materials and Methods.

Table 2: Contribution of Subsites to Transition State Stabilization

subsite	binding mode	$\Delta G_h^{\ddagger}$ (kcal mol^{-1})
−I	3-*O*-Glc*p*	
−II	4-*O*-Glc*p*	−2.1 ± 0.2
−III	4-*O*-Glc*p*	−3.5 ± 0.2
−IV	4-*O*-Glc*p*	−1.2 ± 0.2
−V		−0.11 ± 0.07

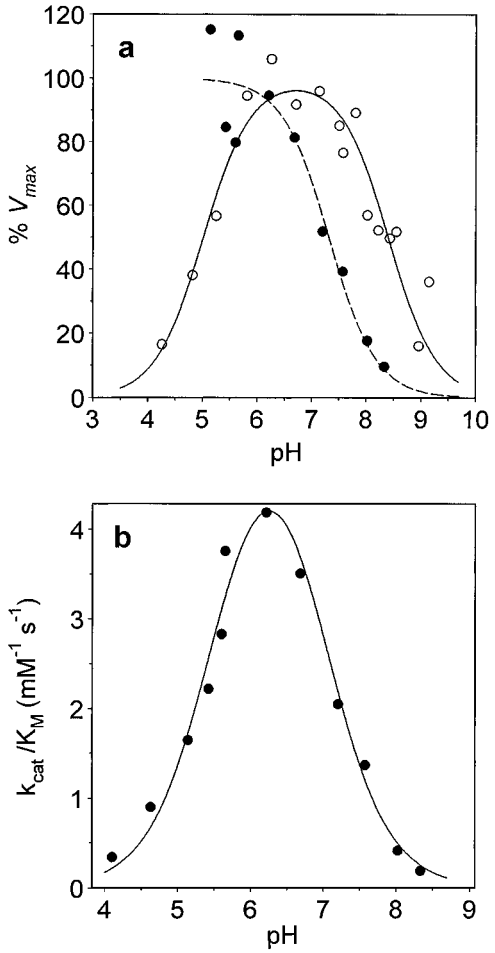

FIGURE 3: pH dependence of the kinetic parameters of 1,3-1,4-β-glucanase with substrates **1c** (●) and barley β-glucan (○). (a) pH profile of k_{cat}, (b) pH profile of k_{cat}/K_M. Conditions: 11 mM citrate−11 mM phosphate buffer for the pH range 4 to 8.3, 11 mM TAPS for the pH range 8−10, 0.1 mM $CaCl_2$, ionic strength to 0.1 M with added KCl, 53 °C. Adjusted parameters are given in Table 3.

1,4-β-glucanase with EAC at pH 6.0 results in complete enzyme inactivation. Semilogarithmic plots of residual activity as a function of time at various reagent concentrations were linear (Figure 4), signifying that the inactivation process obeys pseudo-first-order kinetics.

Table 3: Kinetic pK_a Values of the pH Dependence of Enzyme Activity and Chemical Inactivation of *B. licheniformis* 1,3-1,4-β-Glucanase

	kinetics[a]	k_{cat}/K_M	k_{cat}
substrate			
G4G3G-MU (**1c**)	k_{lim}	5.7 ± 0.6	10.7 ± 0.6
	pK_{a1} (Glu134)	5.5 ± 0.1	<5
	pK_{a2} (Glu138)	7.0 ± 0.1	7.3 ± 0.1
barley β-glucan	k_{lim}		4680 ± 310
	pK_{a1} (Glu134)		5.0 ± 0.2
	pK_{a2} (Glu138)		8.5 ± 0.1
chemical inactivation[b]			
	$(k_{app})_{lim}$	0.092 ± 0.005	
EAC	pK_a	7.0 ± 0.2	

[a] Data on k_{cat}/K_M were fit to eq 4, and data on k_{cat} to eq 3. $(k_{cat}/K_M)_{lim}$ in mM^{-1} s^{-1}, $(k_{cat})_{lim}$ in s^{-1}. Experimental conditions are in Figure 3. [b] Residual activity data were fit to eq 6. $(k_{app})_{lim}$ in min^{-1}. Experimental conditions are in Figure 5.

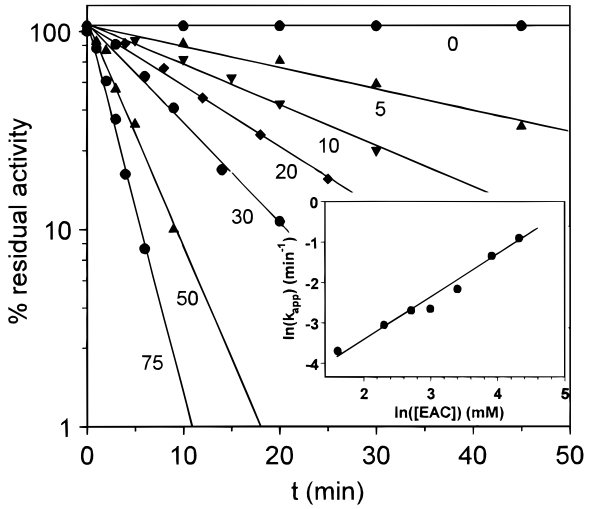

FIGURE 4: Kinetics of enzyme inactivation by EAC in 50 mM MES pH 6.0, 25 °C. The enzyme concentration is 0.7 μM, and reagent concentrations are given in the plot (mM). Residual activity was determined at pH 7.2 with barley β-glucan as substrate after quenching the inactivation reaction with sodium acetate pH 4.7. Inset: ln(k_{app}) *vs* ln[reagent] plot where k_{app} is the pseudo-first-order rate constant of inactivation.

In addition to carboxyl groups, carbodiimides are also capable of modifying tyrosines and cysteines. *B. licheniformis* 1,3-1,4-β-glucanase possesses two cysteine residues that are in a disulfide bond (as observed in the 3D structure and determined by DTNB titration). To check for the interference of tyrosine residues, the modification with tetranitromethane (TNM), specific for Tyr at pH 8.0 (*34*),was studied. An average of 12 ± 1 out of the 18 Tyr in the native protein were modified with an excess of TNM, but only 60−80% reduction in activity was observed. Most of

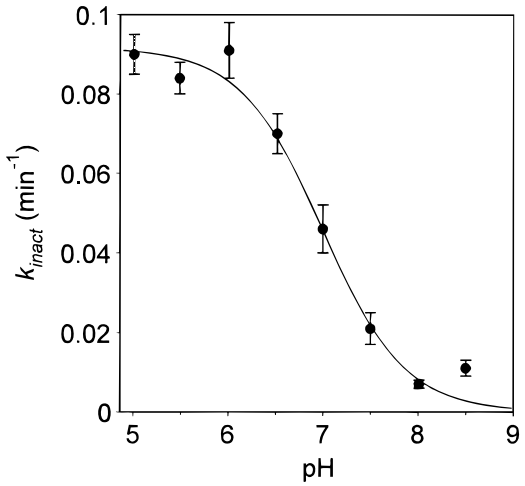

FIGURE 5: pH dependence of the chemical inactivation of 1,3-1,4-β-glucanase with EAC. Conditions: inactivation reactions of 10 μM enzyme with 30 mM EAC in MES/HEPES/4-hydroxy-1-methyl-piperidine buffer at 25 °C; residual activity using **1e** as substrate at pH 7.2, 53 °C. Data were fit to eq 6.

the tyrosine residues located in the binding site cleft might have been modified, decreasing the substrate binding affinity and hence reducing activity, but none is essential for catalysis. Therefore the complete inactivation by EAC is assigned to modification of carboxyl groups.

Analysis of the order of inactivation with respect to EAC by the method of Levy (*35*) (log k_{app} *vs* log[EAC], where k_{app} is the apparent first-order rate constant derived from the time course of the inactivation as shown in Figure 4) yielded a slope of 0.97 ± 0.08 (Figure 4, inset). It indicates that an average of at least one molecule of reagent binds to one molecule of enzyme when inactivation occurs. In consequence, at least the modification of one carboxylic amino acid residue accounts for the observed inactivation. Furthermore, addition of cellobiose (a poor inhibitor of the enzyme) reduced the rate of inactivation in a concentration dependent manner (data not shown), thus suggesting that protection was provided to at least one essential carboxyl group in the active site.

The pH dependence of the inactivation rate constant (k_{app}) at 25 °C using 30 mM EAC in a buffer with constant ionic strength was investigated in the pH range from 4 to 8.5. As shown in Figure 5, k_{app} decreases with increasing the pH. Data were fit to a single ionization process according to eq 6

$$k_{app} = \frac{(k_{app})_{lim}}{1 + 10^{pH-pK_a}} \qquad (6)$$

where $(k_{app})_{lim}$ is the limiting value at low pH, and pK_a corresponds to the kinetic pK_a describing the inactivation process that can be assigned to the essential carboxyl group responsible for the inactivation (Table 3).

DISCUSSION

The oligosaccharides of general structure **1a**−**e** are the first low molecular weight specific substrates of 1,3-1,4-β-glucanases. Although closely related to other chromophoric oligosaccharides previously reported in studies of glycosidases (*26*, *29*, *30*, *36*, *37*), the characteristics of both the enzyme and the designed substrates are quite unique among the previous analyses of endoglucanases: the presence of a single β-1,3 glycosidic bond causes the enzymatic hydrolysis to occur regiospecifically with liberation of the aglyconic chromophore, facilitating both monitoring of the reaction by UV or fluorescence spectroscopy and interpretation of the results on the basis of relatively simple kinetic models. The enzyme-catalyzed hydrolysis of **1d** proceeds with net retention of the anomeric configuration, in agreement with our previous results on the depolymerization of barley β-glucan which identified the enzyme as a retaining *endo*-glycosidase (*3*). Substrates require a minimum G3G-X core structure to be efficiently hydrolyzed by the enzyme because 4-methylumbelliferyl β-glucoside is a very poor substrate. On the other hand, the observed substrate inhibition for **1b**−**e** is consistent with an open binding site cleft where two molecules of a low molecular weight substrate may bind with formation of unproductive ternary complexes. Kinetics with **1a**−**e** indicate an extended carbohydrate binding site cleft composed of four glucopyranose binding subunits on the nonreducing end from the scissile glycosidic bond. Additional analysis by molecular modeling on the X-ray structure of the *B. licheniformis* enzyme showed to be in agreement with this binding cleft arrangement. Based on the crystal structure of the covalent protein−inhibitor complex between H(A16M) 1,3-1,4-β-glucanase and 3,4-epoxybutyl β-cellobioside (*38*), the hexasaccharide G4G4G4G3G4G (**8**) was built into the active site cleft. In a simulated productive binding mode, rotation around the terminal glycosidic bond on the nonreducing end of **8** is not restricted by van der Waals contacts with the protein surface, and the terminal Glc*p* unit lays essentially outside the binding site fully exposed to bulk solvent. The measured contribution of less than 0.1 kcal/mol to transition state stabilization for a virtual subsite−V, is then assigned to unspecific interactions between the edge of the binding cleft and a fifth Glc*p* unit facing the bulk solvent in a loose conformation.

Subsites −II to −IV have a stabilizing effect on the enzyme-carbohydrate transition state complex as determined from k_{cat}/K_M values. Part of this effect might be ground state stabilization of the Michaelis complex since K_M values decrease from the mono to the tetrasaccharide substrates. The calculated $\Delta G^{\ddagger}_{subsite}$ are for 4-*O*-substituted glucopyranose units occupying these subsites. The substrate specificity and cleavage pattern shown by the enzyme on polysaccharides clearly indicate that subsite −I and −II can only accommodate a 3-*O*- and 4-*O*-substituted glucopyranosyl, unit, respectively; no hydrolase activity is observed on cello- and laminarin-oligosaccharides. On the other hand, subsites −III and −IV posses a certain degree of flexibility for the disaccharide motif that can be bound: barley β-glucan locates a cellobiosyl unit in these subsites, while the SIII pneumococcal polysaccharide, a glucan with alternating β-1,3 and β-1,4 glycosidic bonds (*2*), locates a laminaribiosyl unit in the same subsites in the productive binding mode. The determined contribution to transition state stabilization for subsites −III and −IV accomodating a cellobiosyl motif are −3.5 and −1.2 kcal mol^{-1} respectively (Table 2), but the corresponding thermodynamic parameters for a bound laminarin type residue remain to be measured. In addition, recent conformational analysis of β-glucan oligosaccharides containing β-1,3 and β-1,4 linkages (*39*) have shown that two glucopyranose units linked by a β-1,3 bond have the Glc*p* rings in the same orientation, *i.e.* the 6-CH_2OH side chains pointing to the same face (A−A conformation), whereas a

Scheme 1

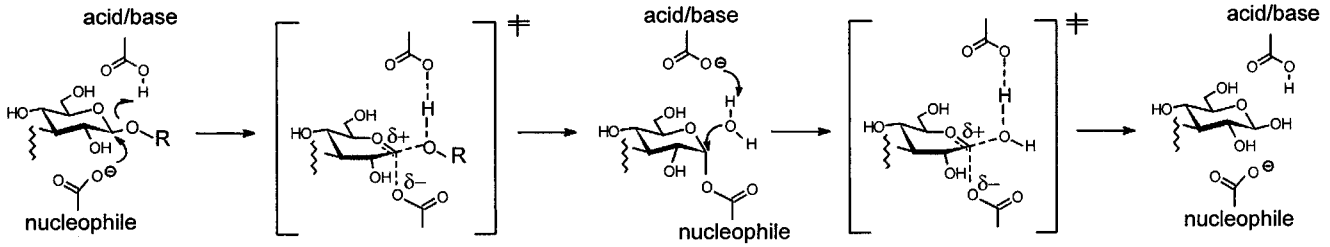

β-1,4 linkage renders both Glc*p* in alternate conformations (B−A conformation), the 6-CH_2OH side chains at approximately 180°. Thus, while the overall spatial orientation of the Glc*p* unit in subsite −III for both cello and laminarin type of residue is essentially the same, subsite −IV can formally bind two different flipped conformations depending on the type of interglycosidic linkage between the two Glc*p* residues. Work is currently in progress to analyze the different interactions that give rise to these distinct binding modes within the same subsite.

The determination of the number of glucopyranose binding subsites from the cleaved glycosidic bond to the reducing end of the oligo/polysaccharide substrate is currently under study using an extended family of β-1,3-1,4-oligosaccharides. However, comparison of the kinetic results obtained with trisaccharide **2a** (G4G3G-OMe), tetrasaccharide **2b** (G4G3G4G-OMe), and the methylumbelliferyl glycoside **1c** (G4G3G-OMU) allow a first qualitative interpretation of the effect in binding and catalysis of a glucopyranose unit located in subsite +I. Assuming similar binding modes for all of the three glycosides, the efficiency of hydrolysis (k_{cat}/K_M) in terms of the leaving group after the enzymatic cleavage follows the order −Glc*p*-OMe > −OMU ≫ −OMe. A difference in free energy of activation of −1.9 kcal mol^{-1} is deduced from the second-order rate constants for the tetrasaccharide **2b** and the methylumbelliferyl glycoside **1c**. However, both substrates show almost identical K_M values (also close to the K_I value for **2a)**, the difference in reactivity being a consequence of an 18-fold increase of k_{cat} for **2b**. These results suggest at this point that subsite +I has a large effect in catalysis, the interactions between subsite +I and the substrate being mainly used to lower the energy of the transition state in the rate-determining step, rather than in the stabilization of the Michaelis complex.

Retaining glycosidases follow a double-displacement mechanism (*40*−*43*) (Scheme 1). The first "glycosidation" step leads to a glycosyl−enzyme intermediate through general acid catalysis in which an acidic amino acid residue protonates the glycosidic oxygen with concomitant C−O breaking of the scissile glycosidic bond via an oxocarbonium ion-like transition state stabilized by the catalytic nucleophile either by electrostatic interaction or covalent bond formation. The second "deglycosidation" step requires the conjugate base of the general acid residue as a general base to promote the attack of a water molecule at the anomeric center. The β-glycose product is formed and the enzyme returns to its initial protonation state. Site-directed mutagenesis has identified E134 and E138 as the essential catalytic residues in the *B. licheniformis* 1,3-1,4-β-glucanase (*10*, *11*). Identification of E134 as the nucleophile is supported by the affinity labeling experiments on the highly homologous *B. amyloliquefaciens* enzyme (*9*), and the X-ray structure of a covalent enzyme−inhibitor complex of the hybrid H(A16M) isozyme (*38*). The assignment of the residue acting as a general acid−base catalyst to E138 was solely based on the fact that, in addition to E134, it was the only carboxylic amino acid residue conserved among the *Bacillus* 1,3-1,4-β-glucanases whose mutation to Gln or Ala yielded inactive enzymes. Moreover, inspection of the X-ray structure (*13*) indicates that E138 is suitably disposed for catalysis at 5.3 Å (O to O) from E134. More recently, a detailed kinetic analysis in which a chemical rescue methodology has been applied to the inactive E138A mutant provides a direct functional evidence of E138 being the general acid−base catalyst (manuscript in preparation). Interpretation of the pH-dependent kinetic data is then analyzed according to this active site model.

The pH dependence of the second-order rate constant k_{cat}/K_M for **1c** reflects the behavior of the uncomplexed (free) enzyme. We attribute the lower pK_a (5.5) to E134 which must be deprotonated to function as a nucleophile, and the higher pK_a (7.0) to E138 which must remain protonated to act as a general acid catalyst. The pH-dependent enzyme inactivation by EAC shows a single ionization curve with a pK_a in the basic limb of 7.0, the same value as that of the higher pK_a on k_{cat}/K_M. Since enzyme inactivation due to chemical modification follows the ionization of an essential carboxylic amino acid residue that reacts in its protonated form, it provides additional support to the assignment of the apparent pK_a of 7.0 to E138 in the free enzyme. This pK_a is abnormally high compared with that of a normal glutamic acid residue (pK_a = 4.4), as is commonly found for the general acid catalyst in retaining glycosidases. Although the interpretation of kinetic pH profiles may not be trivial (*44*), a number of examples in which the ionization of individual residues were determined by direct titration using NMR spectroscopy (*B. circulans* xylanase, ref 45; hen and turkey egg white lysozymes, refs 46 and 47), have confirmed that the apparent pK_a values on well-defined bell-shaped k_{cat}/K_M profiles reflect the ionization of the catalytic residues.

The pK_a in the basic limb of the pH dependence of k_{cat} for **1c** is 7.3. Compounds **1c** and **2b** have the same glyconic structure occupying subsites −I to −III in the productive complex, differing in the leaving group in subsite +I (4-methylumbelliferone *vs* methyl glycoside). Since the deglycosidation step is independent of the leaving group, the larger k_{cat} and k_{cat}/K_M values for **2b** compared to **1c** indicate that the glycosidation step leading to the common glycosyl−enzyme intermediate is rate determining in the hydrolysis of **1c**. In this case, the pK_a of 7.3 in the basic limb of k_{cat} reflects the pH dependence of the first glycosidation step that involves the proton transfer from the general acid residue to the oxygen of the scissile glycosidic bond. Therefore, this pK_a may be assigned to the general acid catalyst in the non-covalent enzyme−substrate Michaelis complex.

Summarizing, we assign the pK_a of 7.0 (on k_{cat}/K_M for **1c** and on the pH-dependent inactivation by EAC) to the general acid catalyst (E138) in the free enzyme. This value is shifted to 7.3 in the enzyme−substrate complex with **1c**, and further shifted to 8.5 when complexed with a polysaccharide substrate (barley β-glucan). This large upward shift of the pK_a may be explained as the result of a more hydrophobic environment of the general acid catalyst due to binding of the substrate and/or to disruption of the hydrogen bond network that stabilizes the carboxylate form in the free enzyme. This effect is substrate-dependent: binding of **1c** locates a 4-methylumbelliferyl aglycon in subsite +I with the concomitant displacement of water molecules that may rise the pK_a of E138; barley β-glucan, on the other hand, is a larger substrate that fills entirely the binding site cleft inducing a larger effect in the enzyme−substrate complex.

APPENDIX

Subsite Mapping Model

The model of extended binding site of depolymerases as an arrangement of subsites, each one accommodating a monomeric substrate unit, was essentially developed independently by Allen and Thoma (*31*, *32*, *48*, *49*) and Hiromi and co-workers (*50*−*53*) and succesfully applied to the description of the enzymatic action of homodepolymerases. The subsite mapping model assumes that the free energy of binding at each subsite is an intrinsic constant, unaffected by binding or absence of binding at any other subsite:

$$\Delta G_{binding} = \sum \Delta G_h - T\Delta S \tag{7}$$

The contribution of each subsite to binding can be written in terms of the kinetic parameters for the hydrolysis of two substrates differing in one monomeric unit as

$$\Delta G_{r,h=n+1} = -RT \ln \frac{K_{r,n+1}}{K_{r,n}} \tag{8}$$

where $K_{r,n}$, $K_{r,n+1}$ are the microscopic Michaelis constants for the productive process involving two substrates of degree of polymerization n and $n+1$. Unfortunately, determination of K_r is not straightforward from the observed steady-state kinetic parameters. It is a known fact that binding to a multisubsite binding cleft of a depolymerase may lead to different positional isomers. Furthermore, the observed uncompetitive substrate inhibition behavior for compounds **1b**−**e** provides strong evidence for multiple binding modes, with only one leading to a productive complex followed by specific hydrolysis at a single glycosidic bond. The general kinetic model shown below accounts for all possible binary and ternary complexes,

$$E + S_n \underset{k_{-1,i,n}}{\overset{k_{+1,i,n}}{\rightleftharpoons}} E{\cdot}S_{i,n} \xrightarrow{k_{2,r,n}} E + P_{n-1} + X$$

$$E{\cdot}S_{i,n} + S_n \overset{K_{i,j,n}}{\rightleftharpoons} E{\cdot}S_{i,n}{\cdot}S_{j,n}$$

where i and j indicate the binding mode (positional isomer), n is the length of the oligosaccharide, r denotes the productive complex, and E and S_n are the free enzyme and substrate. From steady-state considerations, the following relationships can be deduced:

$$1/K_{M,n} = 1/K_{r,n} + \sum_{i \neq r} 1/K_{i,n}$$

$$1/k_{cat,n} = (1/K_{r,n} + \sum_{i \neq r} 1/K_{i,n}) \frac{K_{r,n}}{K_{2,r,n}}$$

$$K_{I,n} = (1/K_{r,n} + \sum_{i \neq r} 1/K_{i,n}) \frac{1}{\sum_j \sum_i 1/K_{i,n} 1/K_{i,j,n}}$$

$$\left(\frac{k_{cat}}{K_M}\right)_n = \left(\frac{k_{2r}}{K_r}\right)_n \tag{9}$$

where $K_{i,n}$ and $K_{i,j,n}$ are the microscopic dissociation constants for the unproductive binary and ternary complexes, which affect the observed K_M, k_{cat}, and K_I parameters but are not accessible from kinetic measurements. Only the second-order rate constant (k_{cat}/K_M) is independent of the eventual formation of unproductive complexes. Equation 7 can be rewritten as

$$\Delta G_{r,h=n+1} = -RT \ln \frac{(k_{cat}/K_M)_{n+1}}{(k_{cat}/K_M)_n} + RT \ln \frac{(k_{2,r})_{n+1}}{(k_{2,r})_n} \tag{10}$$

which, assuming similar hydrolytic coefficients ($k_{2,r}$) for two substrates differing in one monomeric unit, approaches

$$\Delta G_{r,h=n+1} = -RT \ln \frac{(k_{cat}/K_M)_{n+1}}{(k_{cat}/K_M)_n} \tag{11}$$

Using this simplification Hiromi (*50*) initially developed the model of subsite mapping for glycosidases based on the measurement of second-order rate constants for the hydrolysis of substrates of different degrees of polymerization. Hiromi's approach, first succesfully used in the studies of exohydrolases (glucoamylase, ref 51, and β-amylase, ref 54) has been tentatively extended to the analysis of bacterial and fungal α-amylases (*52*, *53*) and 1,4-β-xylanases (*55*, *56*). However, the inherent simplification of the model often leads to subsite binding energies that cannot reproduce the experimental Michaelis constants, and further refinement of the model using hydrolytic coefficients dependent on the degree of polymerization and iterative processes is required (*49*). Assuming that, as a general rule, the intrinsic binding energy is used both for substrate binding and for lowering the free energy of activation in catalysis, the contribution of each subsite to ligand binding cannot be directly calculated with the limited number of substrates described in this study. Additional substrates to map the reducing end of the binding cleft will first be required to complete the analysis and to be able to estimate binding energies using the iterative approach of Allen and Thoma. However, the effect of occupying a subsite h on the second-order rate constant k_{cat}/K_M corresponds to the contribution of that individual subsite to transition state stabilization, and can be expressed by the difference in transition state activation energy between two substrates differing in one glucopyranose unit according to

$$\Delta G^{\ddagger}_{r,h=n+1} = \Delta G^{\ddagger}_{r,n+1} - \Delta G^{\ddagger}_{r,n} = -RT \ln \frac{(k_{cat}/K_M)_{n+1}}{(k_{cat}/K_M)_n} \tag{12}$$

ACKNOWLEDGMENT

We thank Teresa Dot for the enzyme−substrate modeling and Mireia Abel for the chemical modification experiments.

REFERENCES

1. Parrish, F. W., Perlin, A. S., and Reese, E. T. (1960) *Can. J. Chem. 38*, 2094−2104.
2. Anderson, M. A., and Stone B. A. (1975) *FEBS Lett. 52*, 202−207.
3. Malet, C., Jiménez-Barbero, J., Bernabé, M., Brosa, C., and Planas, A. (1993) *Biochem. J. 296*, 753−758.
4. Stone, B. A., and Clarke, A. E. (1992) *Chemistry and Biology of (1→3)-β-glucans*, La Trobe University Press, Bundoora, Australia.
5. Varghese, J. N., Garret, T. P. J., Colman, P. M., Chen, L., Høj, P. B., and Fincher, G. B. (1994) *Proc. Natl. Acad. Sci. U.S.A. 90*, 2785−2789.
6. Borriss, R. (1994) *Curr. Top. Mol. Genet. 2*, 163−188.
7. Henrissat, B. (1991) *Biochem. J. 280*, 309−306.
8. Henrissat, B., and Bairoch, A. (1993) *Biochem. J. 293*, 781−788.
9. Høj, P. B., Condron, R., Traeger, J. C., McAuliffe, J. C., and Stone, B. A. (1992) *J. Biol. Chem. 267*, 25059−25066.
10. Planas, A., Juncosa, M., Lloberas, J., and Querol, E. (1992) *FEBS Lett. 308*, 141−145.
11. Juncosa M., Pons, J., Dot, T., Querol, E., and Planas, A. (1994) *J. Biol. Chem. 289*, 14530−14535.
12. Hahn, M., Olsen, O., Politz, O., Borris, R., and Heinemann, U. (1995) *J. Biol. Chem. 7*, 3081−3088.
13. Hahn, M., Pons, J., Planas, A., Querol, E., and Heinemann, U. (1995) *FEBS Lett. 374*, 221−224.
14. Heinemann, U., Aÿ, J., Gaiser, O., Müller, J. J., and Ponnuswamy, M. N. (1996) *Biol. Chem. 377*, 447−454.
15. Divne, C., Ståhlberg, J., Reinikainen, T., Ruohonen, L., Pettersson, G., Knowles, J. K. C., Teeri, T. T., and Jones, T. A. (1994) *Science 265*, 524−528.
16. Ståhlberg, J., Divne, C., Koivula, A., Piens, K., Claeyssens, M., Teeri, T. T., and Jones, T. A. (1996) *J. Mol. Biol. 264*, 337−349.
17. Wakarchuk, W. W., Campbell, R. L., Sung, W. L., Davoodi, J., and Yaguchi, M. (1994) *Protein Sci. 3*, 467−475.
18. Malet, C., Viladot, J. L., Ochoa, A., Gállego, B., Brosa, C., and Planas, A. (1995) *Carbohydr. Res. 274*, 285−301.
19. Malet, C., Vallés, J., Bou, J., and Planas, A. (1996) *J. Biotechnol. 48*, 209−219.
20. Garegg, P. J., Hultberg, H., and Wallin, S. (1982) *Carbohydr. Res. 108*, 97−101.
21. Planas, A., Juncosa, M., Cayetano, A., and Querol, E. (1992) *Appl. Microbiol. Biotechnol. 37*, 583−589.
22. Laemmli, U. K (1970) *Nature 227*, 680−685.
23. Lloberas, J., Querol, E., and Bernués, J. (1988) *Appl. Microbiol. Biotechnol. 29*, 32−38.
24. Somogyi, M. (1952) *J. Biol. Chem. 195*, 19−23.
25. Nelson, N. (1944) *J. Biol. Chem. 153*, 375−380.
26. van Tilbeurgh, H., Claeyssens, M., and de Bruyne, C. K. (1982) *FEBS Lett. 149*, 152−156.
27. Rosenthal, A. L., and Saifer, A. (1973) *Anal. Biochem. 55*, 85−92.
28. Ellis, K. J., and Morrison, J. F. (1982) *Methods Enzymol. 87*, 405−426.
29. van Tilbeurgh, H., Loontiens, F. C., de Bruyne, C. K., and Claeyssens, M.(1988) *Methods Enzymol. 160*, 45−49.
30. Claeyssens, M., van Tilbeurgh, H., Kamerling, J. P., Berg, J., Vrsanska, M., and Biely, P. (1990) *Biochem. J. 270*, 251−256.
31. Allen, J. D., and Thoma, J. A. (1976) *Biochem. J. 159*, 105−120.
32. Allen, J. D. (1980) *Methods Enzymol. 64*, 248−277.
33. Hoare, D. G., and Koshland, D. E., Jr. (1967) *J. Biol. Chem. 242*, 2447−2453.
34. Sokolovsky, M., Riordan, J. F., and Vallee, B. L. (1966) *Biochemistry 5*, 3582−3589.
35. Levy, H. M., Leber, P. D., and Ryan, E. M. (1963) *J. Biol. Chem. 238*, 3654−3659.
36. Hermans, M. M. P., Kroos, M. A., van Beeumen, J., Oostra, B. A., and Reuser, A. J.J. (1991) *J. Biol. Chem. 266*, 13507−13512.
37. Yang, Y., and Hamaguchi, K. (1980) *J. Biochem. (Tokyo) 87*, 1003−1014.
38. Keitel, T., Simon, O., Borris, R., and Heinemann, U. (1993) *Proc. Natl. Acad. Sci. U.S.A. 90*, 5287−5291.
39. Bernabé, M., Jiménez-Barbero, J., and Planas, A. (1994) *J. Carbohydr. Chem. 13*, 799−817.
40. Koshland, D. E. (1953) *Biol. Rev. 28*, 416−436.
41. Sinnott, M. L. (1990) *Chem. Rev. 90*, 1171−1202.
42. Svensson, B. and Søgaard, M. (1993) *J. Biotechnol. 29*, 1−37.
43. McCarter, J. D., and Withers, S. G. (1994) *Curr. Opin. Struct. Biol. 4*, 885−892.
44. Brocklehurst, K. (1994) *Protein Eng. 7*, 291−299.
45. McIntosh, L. P., Hand, G., Johnson, P. E., Joshi, M. D., Körner, M., Plesniak, L. A., Ziser, L., Wakarchuk, W. W., and Withers, S. G. (1996) *Biochemistry 35*, 9958−9966.
46. Inoue, M., Yamada, H., Yasukochi, T., Kuriki, R., Miki, T., Horiuchi, T., and Imoto, T. (1992) *Biochemistry 31*, 5545−5553.
47. Bartik, K., Redfield, C. and Dobson, C. M. (1994) *Biophys. J. 66*, 1180−1184.
48. Thoma, J. A., Brothers, C., and Spradlin, J. (1970) *Biochemistry 9*, 1768−1775.
49. Thoma, J. A., and Allen, J. D. (1976) *Carbohydr. Res. 48*, 105−124.
50. Hiromi, K. (1970) *Biophys. Res. Commun. 40*, 1−14.
51. Hiromi, K., Nitta, Y., Numata, C., and Ono, S. (1973) *Biochim. Biophys. Acta 302*, 362−375.
52. Iwasa, S., Aoshima, H., Hiromi, K., and Hatano, H. (1974) *J. Biochem. 75*, 969−978.
53. Suganuma, T., Matsuno, R., Ohnishi, M., and Hiromi, K. (1978) *J. Biochem. 84*, 293−316.
54. Kato, M., Hiromi, K., and Morita, Y. (1974) *J. Biochem. (Tokyo) 75*, 565−576.
55. Biely, P., Kratky, Z., and Vrsanska, M. (1981) *Eur. J. Biochem. 119*, 559−564.
56. Biely, P., Vrsanska, M., and Gorbacheva, I. V. (1983) *Biochim. Biophys. Acta 743*, 155−161.

BI9711341